

The VIRMOS-VLT Deep Survey: a Progress Report

O. LE FÈVRE¹, G. VETTOLANI², D. MACCAGNI³, J.-P. PICAT⁴, B. GARILLI³, L. TRESSE¹, C. ADAMI¹, M. ARNABOLDI¹⁰, S. ARNOUITS¹, S. BARDELLI⁵, M. BOLZONELLA³, D. BOTTINI¹¹, G. BUZZARELLO¹⁰, S. CHARLOT⁶, G. CHINCARINI⁷, T. CONTINI⁴, S. FOUCAUD¹, P. FRANZETTI¹¹, L. GUZZO⁷, S. GWYN¹, O. ILBERT¹, A. IOVINO⁷, V. LE BRUN¹, M. LONGHETTI⁵, C. MARINONI¹, G. MATHEZ, A. MAZURE¹, H. MCCRACKEN⁵, Y. MELLIER⁸, B. MENEUX¹, P. MERLUZZI¹⁰, S. PALTANI¹, R. PELLÒ⁴, A. POLLO⁷, M. RADOVICH¹⁰, P. RIPPEPI¹⁰, D. RIZZO⁷, R. SCARAMELLA⁹, M. SCODEGGIO³, G. ZAMORANI⁵, A. ZANICHELLI⁵, E. ZUCCA⁵

¹Laboratoire d'Astrophysique de Marseille, France; ²Istituto di Radio Astronomia, Bologna, Italy; ³Istituto di Fisica Cosmica e Tecnologie Relative, Milan, Italy; ⁴Observatoire Midi-Pyrénées, Toulouse, France; ⁵Osservatorio Astronomico di Bologna, Italy; ⁶Max Planck Institute für Astronomie, Garching, Germany; ⁷Osservatorio Astronomico di Brera, Italy; ⁸Institut d'Astrophysique de Paris, France; ⁹Osservatorio Astronomico di Roma, Italy; ¹⁰Osservatorio Astronomico di Capodimonte, Naples, Italy; ¹¹Istituto di Astrofisica Spaziale e Fisica Cosmica CNR, Milano, Italy

Introduction

The VIMOS instrument has been successfully commissioned at the VLT Mepical in 2002, and is now open to the community, with a first set of observations for General Observers scheduled in Period 71. From the start, VIMOS has been designed with the goal to undertake large, deep surveys of the distant universe. VIMOS is capable of an impressive multiplexing capability: up to 1000 objects can be measured simultaneously [1], which allows to assemble large datasets of faint objects in a short time.

The VIRMOS consortium has defined the *VIRMOS-VLT Deep Survey* (VVDS), as a major programme to study the evolution of galaxies, clusters, large-scale structures, and AGNs, over more than 90% of the current age of the universe [2]. The survey aims to observe more than 100,000 objects in the distant universe $0 < z < 5$, which will allow a solid knowledge of the luminous content of the universe at early epochs, and its evolution, based on large statistical samples.

We describe here the start of the survey with the first guaranteed night observations which have been carried out in the October-December 2002 time frame. The general survey strategy,

performances, and first results are presented.

VVDS Outline

The goal of the VIRMOS deep redshift survey is to study the evolution of galaxies, AGNs, and large-scale structures, over a redshift range $0 < z < 5+$. The requirement is to be able to analyse the basic properties such as the luminosity function or spatial correlation function of the galaxy population, as a function of galaxy type or local density, in each of several time steps covering the redshift range of interest.

We are therefore planning to observe the following magnitude-limited samples:

1. "Wide" survey: more than 10^5 galaxies with redshifts measured to $I_{AB} = 22.5$ (redshift up to $z \sim 1.3$), it will be conducted in 5 fields identified in Table 1.

2. "Deep" survey: more than 4×10^4 galaxies with redshifts to $I_{AB} = 24$ (redshift up to $z \sim 5$) conducted in the 0226-04 field.

3. "Ultra deep survey": more than 10^3 galaxies with redshifts to $I_{AB} = 25$ conducted in the 0226-04 field.

The spectroscopic samples will be observed with $R \sim 210$ in a first pass. A subsample of 10,000 galaxies will then be selected for spectroscopy at a resolution $R \sim 2500-5000$ to allow the study

of the evolution of the fundamental plane, and perform a detailed analysis of the spectro-photometric properties of galaxies.

Four fields in addition to the Chandra Deep Field South are targeted during the course of the survey. Each field is $2 \times 2 \text{ deg}^2$ for the "wide" survey, and 1.3 deg^2 for the "Deep" survey. Extensive imaging has been carried out using the CFHT12K camera, the ESO 2.2-m WIF1, and the NTT-SOFI to assemble a sample of around 2 million galaxies with BVRI photometry, with smaller subsets having in addition U and/or K' photometry [3].

The complete photometric survey gives access to a volume of the universe which is equivalent to the 2DF redshift survey, although at a much higher mean redshift of $z \sim 1$.

First Observations

The ESO Director General has granted the VIRMOS consortium the early use of guaranteed time in the period October-December 2002, immediately following the last commissioning period in September, interleaved with periods of "Paranalization". This approach had a double advantage: to ESO because the consortium committed to technically attend to the instrument with its own

Table 1: VVDS fields

Field	Alpha (2000)	Delta (2000)	Survey area (deg ²)	Survey mode	Observed in Oct.-Dec.2002
0226-04	02h26m00.0s	-04°30'00"	1.3 (Deep) 4 (Wide)	Wide, Deep, Ultra-deep	20 deep pointings, 9188 slits
CDFS	03h32m28.0s	-27°48'30"	0.1 (Deep)	Deep, IFU, early community release	5 deep pointings, 1 deep IFU pointing, 2109 slits
1003+01	10h03m39.0s	+01°54'39"	4 (Wide)	Wide	7 pointings, 2595 slits
1400+05	14h00m00.0s	+05°00'00"	4 (Wide)	Wide	
2217+00	22h17m50.4s	+00°24'27"	4 (Wide)	Wide	17 pointings, 6849 slits

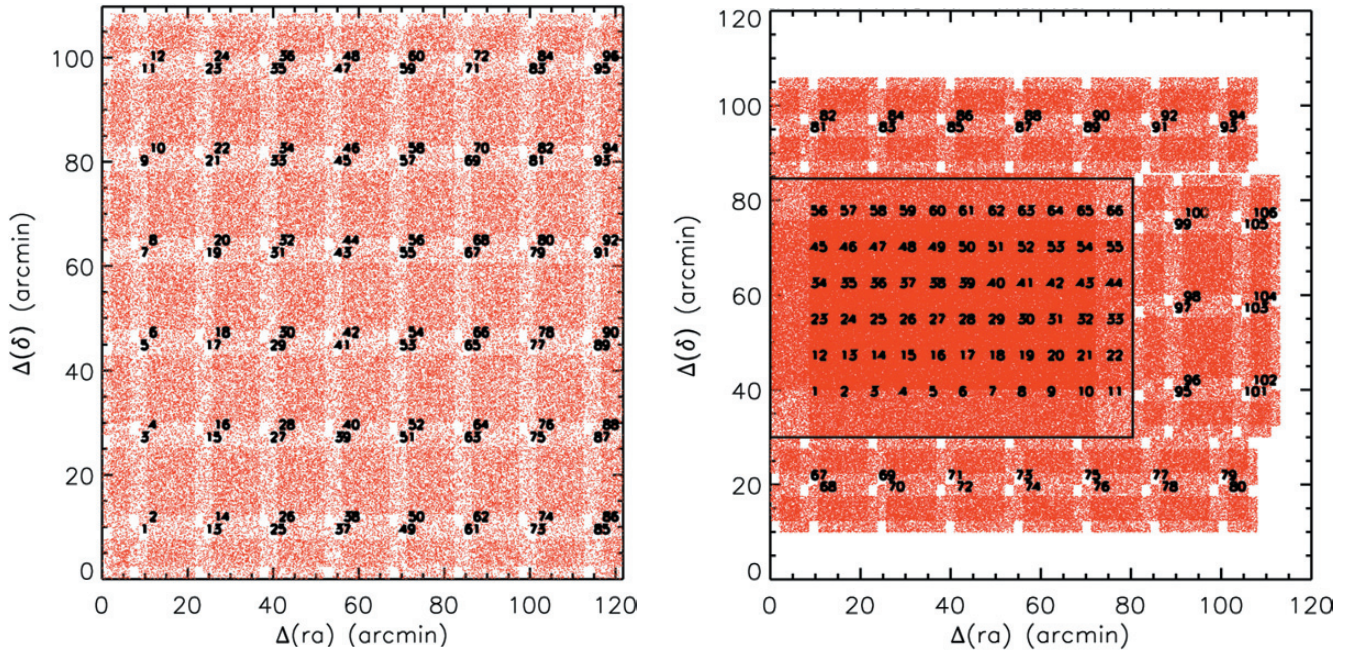


Figure 1: The distribution of the 96 VIMOS pointings for the VVDS-Wide fields (left) and 66 VVDS-Deep pointings (central area, right) and 40 VVDS-Wide pointings in the 0226-04 area. Each pointing of 4 quadrants is labelled and the area covered is shaded in red, with a density increasing at each passage. Targets are selected only in the shaded areas. The spatial selection function for the VVDS-Wide is easy to model and correct for. Carefully selected offset patterns allow to cover an area of 1.3 deg^2 in the 0226-04 Deep area with a smooth spatial selection function totalling 4 passes of VIMOS.

support staff to solve pending problems which may have occurred, therefore making the instrument more reliable; and to the consortium because of the ability of an early start of the VVDS.

Two observing periods have been allocated to the consortium: 29 October – 11 November (14 nights) and 27 November – 11 December (15 nights). The first observing run was blessed with excellent weather, only 2 nights were lost due to high-level clouds, while during the second period strong north winds prevented us from observing dur-

ing 8 nights. In total, the equivalent of 19 dark short summer nights benefited from clear weather and nominal Paranal seeing. While some of the consortium observers had their first time ever on the instrument during this time, the training was smooth and quick. The team made its utmost to ensure that the instrument was ready for each night of observation. As anticipated, we had to face some technical problems, related in particular to the occasional failure of a mask or grism insertion, these were addressed during the day with the con-

sortium technical staff. Less than one night was lost to instrument problems in these first observing runs.

The preparation of masks for the nights of observations has been challenging but smooth, especially during consecutive long periods of nice weather, when up to 6 sets of 4 masks with more than 500 slits in each set had to be manufactured during the day with the Mask Manufacturing Machine [4]. The observing time has been balanced between long integration on the deep survey, and short integration on the

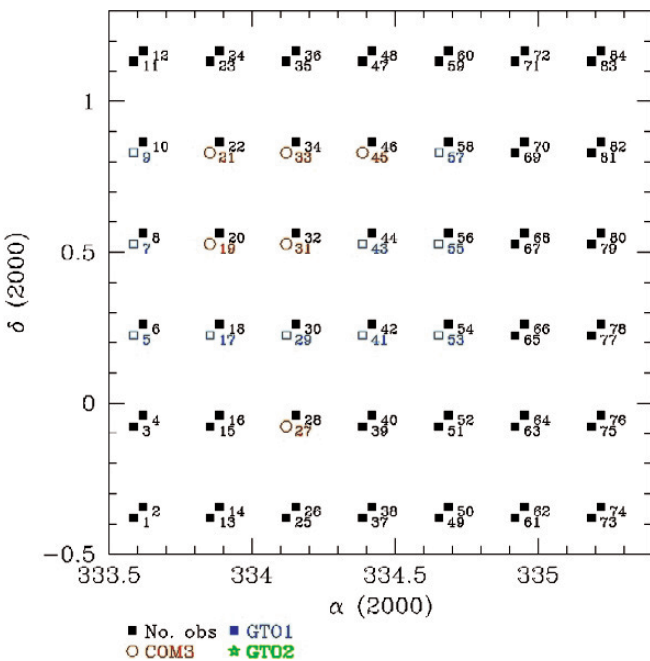


Figure 2: Pointings observed in the 1003+01 VVDS-Wide in the fall 2002.

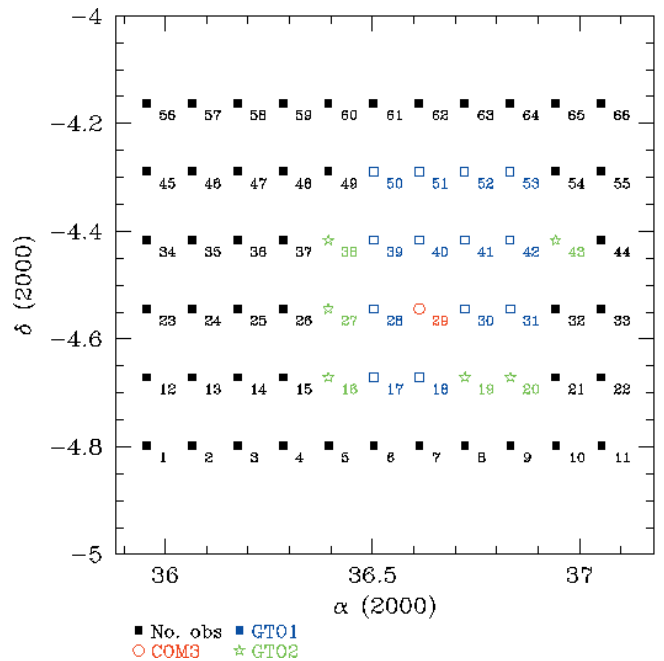


Figure 3: Pointings observed in the 0226-04 VVDS-Deep in the fall 2002.

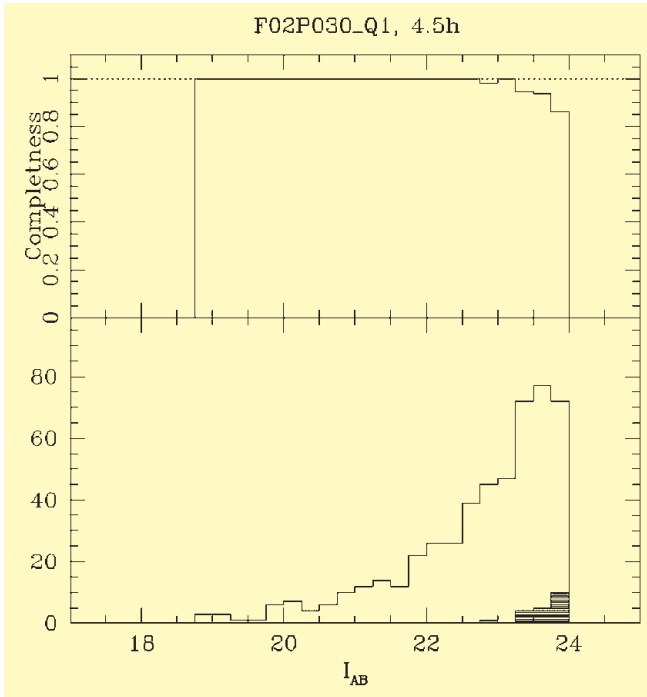


Figure 4: Completeness measurement vs. magnitude in the quadrant 1 of the F02P030-Deep pointing, defined as the ratio of objects with secure redshift identification to the total number of objects observed without instrumental bias (top), and the corresponding magnitude distribution with the objects for which no redshift could be measured, indicated as the shaded histogram (bottom).

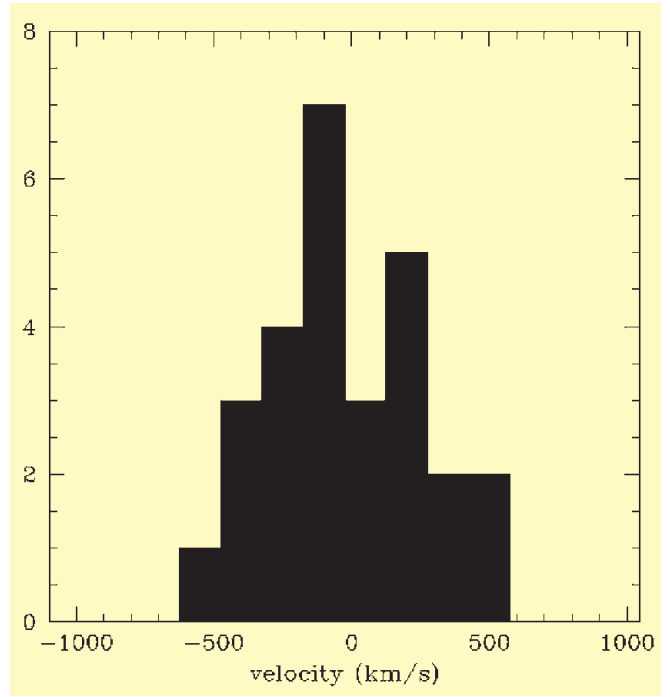


Figure 5: Velocity accuracy: comparison of redshifts measured independently on the same galaxies from two different mask datasets. The error in velocity measurement accuracy is 270 km/s rms for the LRRed grism and 1 arcsec slits.

wide survey. The strategy adopted had been tested during commissioning and is recommended for all MOS observations: because of the strong CCD fringing above 8200 Å, sequences of observations were acquired moving the objects along the slits. This allows to compute the fringing pattern in each slit,

and remove it for an improved sky and fringing correction. For the wide survey, we used an offset pattern 0, -0.7, -1.4, +0.7, +1.4 arcsec from the reference position, with 5 exposures of 9 minutes each, while for the deep survey we used an offset pattern 0, -0.8, -1.6, +0.8, +1.6 arcsec, repeating twice this pattern for

a total of 10 × 27 minutes exposure.

The VVDS has a set of carefully designed pointings (one pointing is one position of VIMOS on the sky with all four quadrants), to minimize the spatial bias applied by the non-contiguous geometry of the instrument. In the wide survey, we carry out two passes of

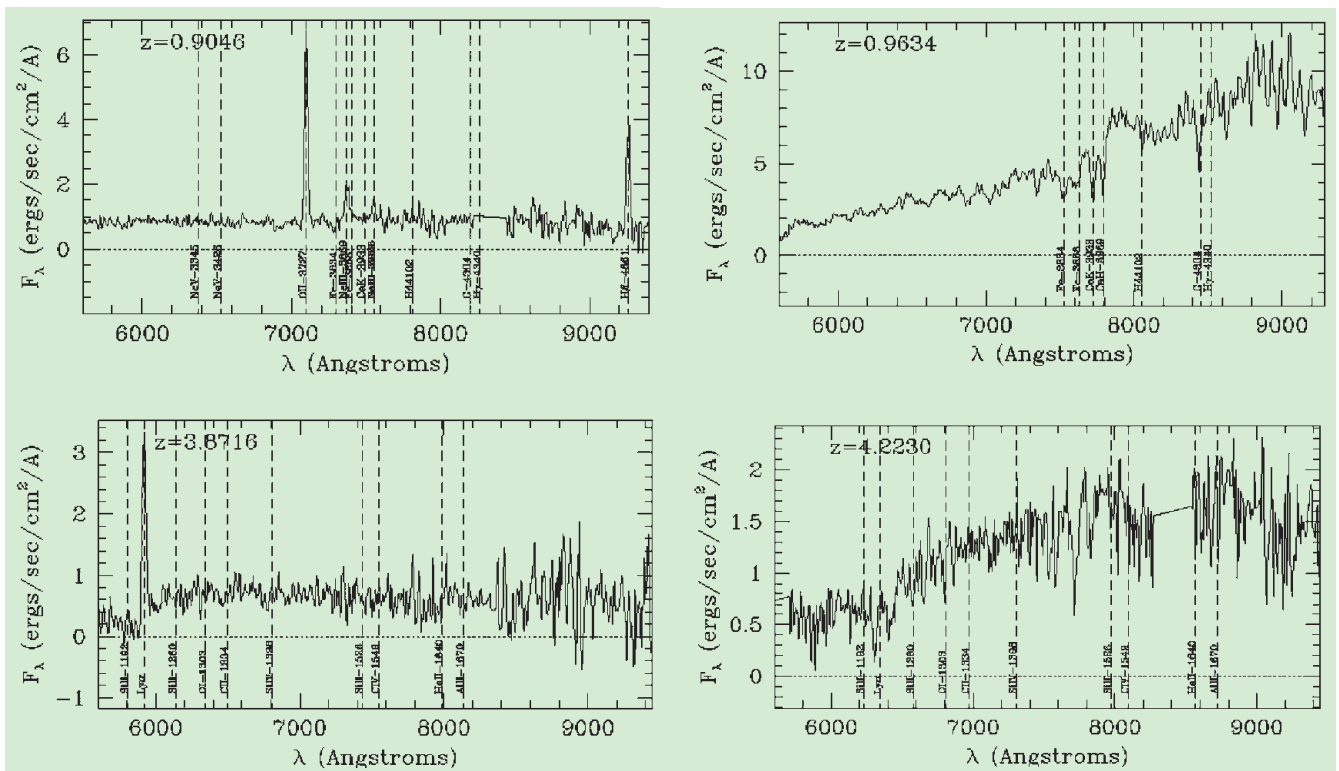


Figure 6: Sample spectra from the first VVDS observations.

VIMOS on the same sky area, offset by (2.2) arcminutes. This ensures that more than 50% of the $I_{AB} = 22.5$ objects are observed on average, with a smooth spatial sampling function which is easy to model (Fig. 1), and to correct for, e.g. for the computation of the correlation function.

For the VVDS Deep, the set of pointings allows for a continuous spatial sampling of the area, with 4 VIMOS passes at any sky location (Fig. 1).

A total of 24 wide pointings have been observed in the 2217+00 and 1003+01 fields, for a total of 9444 slits (Fig. 2), and 25 deep pointings have been observed in the 0226-04 (Fig. 1) and CDFS fields for a total of 11,297 slits.

First Results

The data processing is now in full swing, with 4 teams processing the data in parallel. Each pointing is processed twice: the automated data processing pipeline VIPGI is applied, and the product is distributed to two teams/reducer to extract the redshifts independently. A dedicated tool has been developed to automatically measure redshifts. At this time we examine spectra one by one for redshift measurements proposed by the KBRED tool. Although this process is somewhat long and tedious, it allows one person to process a set of 4 masks with ~ 500 slits in a few working days. Careful data quality assessment is made for each mask, checking the wavelength and flux calibrations.

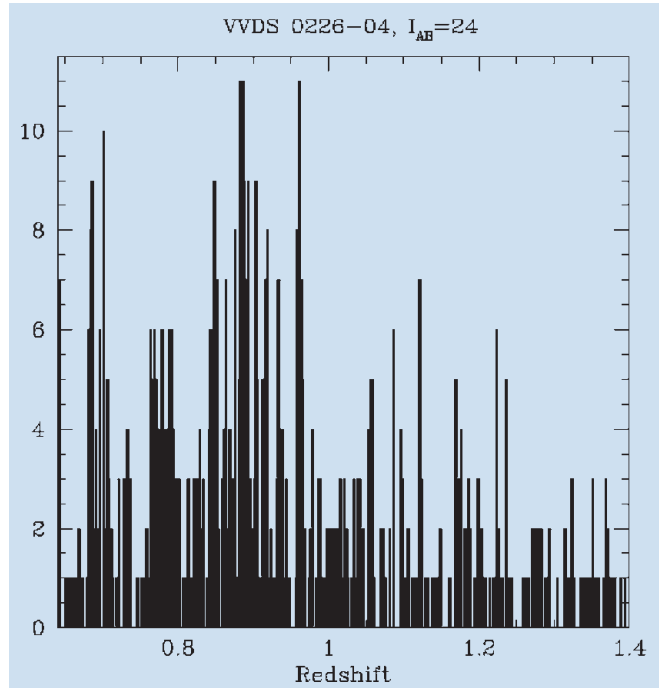
The quality of spectra is as expected. We are experiencing a completeness better than 90% of the overall sample

Figure 7: Redshift distribution of galaxies around $z \sim 1$ in the 0226-04 VVDS-Deep area. This is assembled from 3 pointings, and clearly shows dense peaks and empty regions.

for both the wide and deep surveys (Fig. 4). The velocity accuracy has been estimated from independent redshift measurements of the same galaxies in two different pointings, it is ~ 270 km/s rms as derived from a sample of 27 galaxies (Fig. 5). Examples of spectra are shown in Figure 6.

We have performed test observations for the $R \sim 2500$ follow-up observations which will be carried out on objects selected from the low-resolution survey. Spectra of $z \sim 1$ galaxies with emission lines like [OII] (Fig. 8) show that the measurement of the velocity dispersion in galaxies will be possible to a level of ~ 30 km/s.

In the VVDS-Deep pointings, we find that 10% of the objects are stars, 0.7% QSOs, since no pre-selection has been made besides the I-band limited sample. The fraction of stars is higher at about 15–20% in the VVDS-Wide. The



mean redshift is 0.55 for the VVDS-Wide and 0.8 for the VVDS-Deep. The redshift distribution for each pointing now shows the classical succession of high density peaks and low density areas (Fig. 7).

Conclusion

The VVDS survey is now proceeding with a first set of successful observations. Upon final processing of the more than 20,000 spectra acquired so far, and taking into account the fraction of stars and the completeness, the yield of secure redshift measurements should amount to $\sim 15,000$ for this first set of observations. This will allow for a first computation of the luminosity function and to map the distribution of galaxies down to $I_{AB} = 24$, from a sample free of selection effects.

The raw IFU data obtained on the Chandra Deep Field South is available on-line (<http://www.oamp.fr/virmos>), and we will make a public release of the Chandra Deep Field South MOS data (1D calibrated spectra and redshift measurements) in this same field as soon as the processing is completed.

References

- [1] Le Fèvre, O., et al., *The Messenger*, September 2002.
- [2] Le Fèvre, O., Vettolani, G., Maccagni, D., Mancini, D., Mazure, A., Mellier, Y., Picat, J.P., et al., astro-ph/0101034, ESO Astrophysics Symposia Series "Deep Fields", Cristiani, Renzini, Williams, Eds., Springer, p. 236.
- [3] Le Fèvre, O., Mellier, Y., McCracken, H.J., Arnaboldi, M., et al., 2000, A.S.P. Conf. Series, Clowes, Adamson, and Bromage Eds., vol. 232, p. 449.
- [4] Conti, G., Mattiaini, E., Maccagni, D., Sant'Amrogio, E., Bottini, D., Garilli, B., Le Fèvre, O., Saisse, M., Voët, C., et al., 2001, *PASP*, 113, 452.

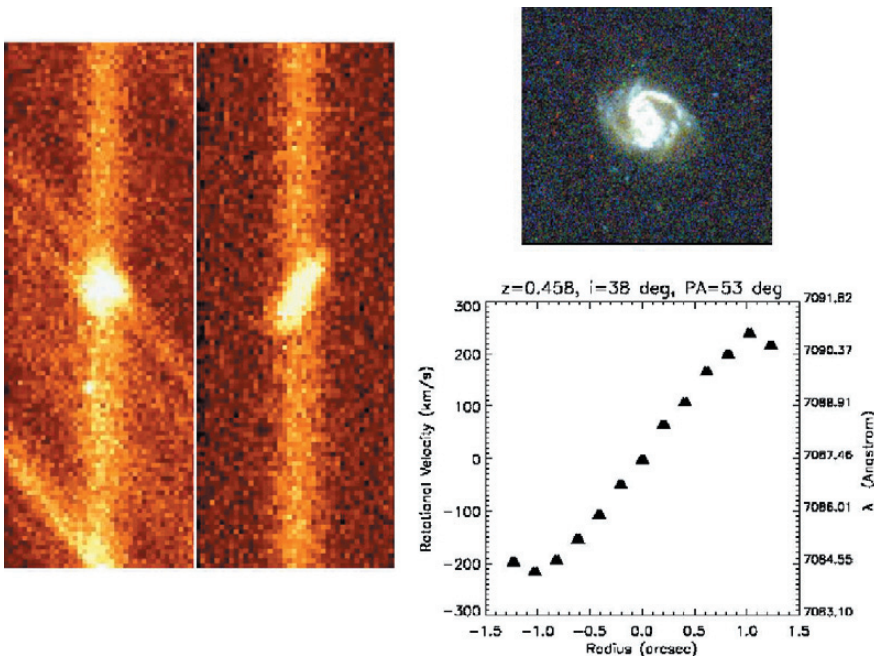


Figure 8: Velocity curve of a galaxy at $z = 0.458$ from observations in the HRRED grism ($R \sim 2500$) of the $H\beta$ line. Left: raw spectrum obtained with a slit cut by the laser machine tilted on the major axis of the galaxy, and corrected spectrum after sky subtraction and wavelength straightened. Right: velocity curve obtained after correction of the inclination angle of the galaxy. Top right: image obtained with HST/ACS (GOODS-CDFS public data).